Am J Physiol Cell Physiol 293: C1687–C1697, 2007.
First published February 7, 2007; doi:10.1152/ajpcell.00189.2006.

Thiol-oxidant monochloramine mobilizes intracellular Ca^{2+} in parietal cells of rabbit gastric glands

Breda M. Walsh, Haley B. Naik, J. Matthew Dubach, Melissa Beshire, Aaron M. Wieland, and David I. Soybel

Department of Surgery, Brigham and Women's Hospital and Harvard Medical School, Boston, Massachusetts

Submitted 15 April 2006; accepted in final form 27 January 2007

Walsh BM, Naik HB, Dubach JM, Beshire M, Wieland AM, Soybel DI. Thiol-oxidant monochloramine mobilizes intracellular Ca^{2+} in parietal cells of rabbit gastric glands. *Am J Physiol Cell Physiol* 292: C1687–C1697, 2007. First published February 7, 2007; doi:10.1152/ajpcell.00189.2006.—In *Helicobacter pylori*-induced gastritis, oxidants are generated through the interactions of bacteria in the lumen, activated granulocytes, and cells of the gastric mucosa. In this study we explored the ability of one such class of oxidants, represented by monochloramine (NH_2Cl), to serve as agonists of Ca^{2+} accumulation within the parietal cell of the gastric gland. Individual gastric glands isolated from rabbit mucosa were loaded with fluorescent reporters for Ca^{2+} in the cytoplasm (fura-2 AM) or intracellular stores (mag-fura-2 AM). Conditions were adjusted to screen out contributions from metal cations such as Zn^{2+}, for which these reporters have affinity. Exposure to NH_2Cl (up to 200 μM) led to dose-dependent increases in intracellular Ca^{2+} concentration ($[Ca^{2+}]_i$), in the range of 200–400 nM above baseline levels. These alterations were prevented by pretreatment with the oxidant scavenger vitamin C or a thiol-reducing agent, dithiothreitol (DTT), which shields intracellular thiol groups from oxidation by chlorinated oxidants. Introduction of vitamin C during ongoing exposure to NH_2Cl arrested but did not reverse accumulation of Ca^{2+} in the cytoplasm. In contrast, introduction of DTT or *N*-acetylcysteine permitted arrest and partial reversal of the effects of NH_2Cl. Accumulation of Ca^{2+} in the cytoplasm induced by NH_2Cl is due to release from intracellular stores, entry from the extracellular fluid, and impaired extrusion. Ca^{2+}-handling proteins are susceptible to oxidation by chloramines, leading to sustained increases in $[Ca^{2+}]_i$. Under certain conditions, NH_2Cl may act not as an irritant but as an agent that activates intracellular signaling pathways. Anti-NH_2Cl strategies should take into account different effects of oxidant scavengers and thiol-reducing agents.

calcium; *Helicobacter pylori*; oxidative stress

IN HUMAN TISSUES AND EXPERIMENTAL models of *Helicobacter* gastritis, reactive species play well-recognized roles in inflammation-induced toxicity to microbes and injury to the "bystander" gastric mucosa (12, 29, 50, 55, 56). In a variety of tissues, exposures to oxidants activate diverse intracellular signaling pathways (51). Among these signals are the intracellular accumulation of Ca^{2+} and Zn^{2+} in their labile forms (10, 17, 19, 49, 54). When uncontrolled, such divalent cation accumulation can exacerbate tissue injury (14, 42). When released in moderation, such signals may be protective (3, 48, 51). To more clearly explore the implications of such signals, it is important to clearly delineate their magnitude and temporal characteristics.

In this study, we explored the ability of one class of oxidants, the chloramines, to cause disturbances in intracellular homeostasis of Ca^{2+} and Zn^{2+} in epithelial cells of a primary functional unit, the secretory gland of gastric mucosa. The prototype in this class of oxidants, monochloramine (NH_2Cl), is produced through the reaction of neutrophil-derived hypochlorous acid (HOCl) with bacteria-derived ammonia (NH_3) (21, 53). Monochloramine is cell permeant and relatively stable in aqueous environments (20, 21). Molecular species that consume or neutralize the oxidant Cl· of chloramine species include (but are not limited to) glutathione and other peptides and proteins in which thiol (-SH) groups or clusters are integral to structure or enzymatic functions (11, 44). Recent studies have implicated such thiol groups in structural proteins and enzymes that regulate cell uptake and intracellular movements of Ca^{2+} and Zn^{2+} (1, 37, 38, 47). These considerations led us to hypothesize that exposure of gastric epithelial cells to NH_2Cl would elicit a distinct profile of disturbances in intracellular Ca^{2+} and Zn^{2+} through oxidation of thiol groups on proteins that bind and transport divalent cations.

Recently, we documented (10) such oxidant-induced disturbances in intracellular Ca^{2+} concentrations ($[Ca^{2+}]_i$) in epithelial cells of the colon mucosa, a specialized tissue in which NH_2Cl would be generated by the interaction of activated neutrophils and NH_3-producing bacteria. In the present study we used fluorescence-based reporters fura-2 and mag-fura-2 to examine, in detail, the mobilization of Ca^{2+} in parietal cells of the gastric gland during exposure to oxidants such as NH_2Cl. The parietal cell was chosen for study, in part, because its secretory dysfunction is an early consequence of acute, fulminant *Helicobacter pylori* gastritis (25, 40). In addition, the gastric parietal cell is highly enriched in mitochondria (27) and thus has the potential for use in evaluating cell energetics and classic pathways of apoptosis during oxidant-induced disturbances in $[Ca^{2+}]_i$ and intracellular Zn^{2+} concentration ($[Zn^{2+}]_i$). Moreover, it is feasible to monitor the emptying and filling of intracellular Ca^{2+} stores in the gastric parietal cell with fluorescent reporters such as mag-fura-2 (31, 32). This approach offered the opportunity for a detailed examination of oxidant-induced disturbances in store emptying and repletion.

In this study, we used calcium ion reporters (fura-2 and mag-fura-2) to monitor $[Ca^{2+}]$ in the cytoplasm and content within intracellular stores, respectively. It is well recognized that high-affinity calcium reporters are also responsive to heavy metals such as Zn^{2+}, often with much higher affinity (2). Thus, initially, we performed studies to demonstrate that a heavy

Address for reprint requests and other correspondence: D. I. Soybel, Dept. of Surgery, Brigham and Women's Hospital, 75 Francis St., Boston, MA 02115 (e-mail: dsoybel@partners.org).

The costs of publication of this article were defrayed in part by the payment of page charges. The article must therefore be hereby marked "*advertisement*" in accordance with 18 U.S.C. Section 1734 solely to indicate this fact.

metal chelator [*N,N,N′,N′*-tetrakis-(2-pyridylmethyl)ethylenediamine, TPEN] may be used to screen out contributions from metal cations such as Zn^{2+}, without impairing responses of the fluorescent reporters to calcium signals in the physiological range (100 nM to 1 μM). After these initial validation studies, the primary goal of our studies was to determine the magnitude and time course of Ca^{2+} accumulation in response to NH_2Cl. A second goal was to determine the sources and possible mechanisms behind that accumulation. Our third goal was to determine whether the effectiveness of different antioxidant strategies would depend on the timing of their administration relative to the exposure to NH_2Cl.

MATERIALS AND METHODS

Gland isolation. Animal use protocols, including anesthesia, euthanasia, and experimental procedures, were approved by an independent review board in the Harvard Medical School, which oversees animal use at Brigham and Women's Hospital. New Zealand White rabbits (~2 kg) were anesthetized and underwent midline laparotomy. The aorta was cannulated and perfused retrograde with warmed (37°C) phosphate-buffered saline solution (mM: 150 NaCl, 0.6 NaH_2PO_4, 3 K_2HPO_4, 1 $CaCl_2$, and 1 $MgCl_2$ with 100 μM cimetidine, adjusted to pH 7.4 with HCl/NaOH). The gastric mucosa was separated from the underlying muscularis. Isolated glands were prepared with a modification (8) of previously published methods (4, 31). Collagenase type I (Sigma, St. Louis, MO) was used for ~60-min digestion with BSA in Dulbecco's modified Eagle's medium (DMEM, Sigma; with 100 μM cimetidine, pH 7.4). Glands were used within 8 h of isolation.

Dye loading. Fura-2 AM and mag-fura-2 AM (Molecular Probes, Eugene OR) were diluted in dimethyl sulfoxide to 1.0 mM. Glands were loaded at room temperature in DMEM (100 μM cimetidine, pH 7.4) with dye concentrations between 4 and 8 μM for 25 min. Subsequently, glands were rinsed several times in dye-free DMEM, mounted on glass coverslips, and then transferred to the microscope stage (Olympus IMT-2 or Nikon TE-2000), where they were perfused with Ringer solution (mM: 145 NaCl, 2.5 KH_2PO_4, 1.0 $MgSO_4$ or 1.0 $MgCl_2$, 1.0 $CaCl_2$, 10 HEPES, and 10 glucose, pH 7.4) at room temperature.

Gland permeabilization. In some cases, glands were permeabilized with digitonin (31, 32) after they had been mounted on coverslips and were under microscopic observation. After an initial rinse and stabilization in Ringer solution, glands were perfused with intracellular buffer [ICB; mM: 125 KCl, 25 NaCl, 0.3 $CaCl_2$, 0.5 $MgCl_2$, 10 HEPES, 0.5 Na_2ATP, and 0.5 ethylene glycol-bis(β-aminoethyl ether)-*N,N,N′,N′*-tetraacetic acid (EGTA), pH 7.25, room temperature] containing 10 μM digitonin.

Imaging and ratiometric measurements. Simultaneous fluorescence measurements were obtained within each gland, in 6–10 individual cells. Fura-2- and mag-fura-2-loaded cells were excited alternately at 340 and 380 nm with a T.I.L.L. Photonics Polychrome IV system (Martinsried, Germany). Emitted light was collected at 520 ± 15 nm after alternating excitation; the ratio of emission intensities provides an index of the Ca^{2+} concentration in the cytoplasm (fura-2) or subcellular compartments in permeabilized glands (mag-fura-2) (31, 32, 41). Digital images of glands were captured with a digital charge-coupled device camera (Hamamatsu ORCA-ER). Images were processed with compatible software (Universal Imaging, Downington, PA) to yield background-corrected pseudocolor images reflecting the 340 nm-to-380 nm ratio. Images were acquired every 10 s to minimize photobleaching. Contributions of autofluorescence were measured and taken into account, although these contributions were generally negligible because of bright staining of glands.

Preparation of monochloramine. Monochloramine (NH_2Cl) was prepared as described previously (10, 20, 21). Briefly, a 200-μl solution containing 500 mM NaOCl in water was added dropwise to 10 ml of 20 mM NH_4Cl and 5 mM Na_2HPO_4 in water at 0°C. This procedure resulted in a 5 mM NH_2Cl solution. Use of concentrated NH_2Cl solutions was completed within 6 h of preparation, as we observed that it remained stable in Ringer solution at concentrations ranging from 50 to 200 μM with <10% loss of absorbance at 242 nm. The concentrated solution was kept on ice and then diluted to the final concentration just before each experiment. Taurine monochloramine (TaurNHCl) was generated under similar conditions by including taurine instead of NH_4Cl in the reaction mixture (20, 21). Concentrations were verified by measuring absorbance in a UV spectrophotometer at 242, 292, and 252 nm for NH_2Cl, HOCl, and TaurNHCl, respectively. [NH_2Cl], [HOCl], and [TaurNHCl] were then quantified with molar extinction coefficients reported previously (53).

Western blot. Protein determinations were made with the Bradford protein assay (Sigma). SDS-PAGE was performed according to Laemmli (36). Samples were boiled for 5 min. For Western blotting, primary (mouse anti-human) antibodies were diluted in Tris-buffered saline-0.1% Tween 20 as follows: anti- sarco(endo)plasmic reticulum Ca^{2+}-ATPase (SERCA)2 1:1,000 (clone C2C12, ABR-Affinity Bioreagents), anti-Na^+/Ca^{2+} exchanger (NCX) 1:1,000 (clone 2A7-A1, ABR-Affinity Bioreagents), and anti-Na^+-K^+-ATPase, α_{1c}-subunit, 1:5,000 (Chemicon). Goat anti-mouse secondary antibody was used at 1:2,000 dilution. Blocking of nitrocellulose was done in 3% nonfat milk in Tris-buffered saline. Horseradish peroxidase was detected by chemiluminescence (LumiGLO, KPL; www.KPL.com), and the signal was visualized on Kodak Bio-Max X-ray film.

Additional reagents and methods. Nigericin, ionomycin, digitonin, DTT, and ascorbic acid (vitamin C, VitC) were obtained from Sigma. TPEN was obtained from Molecular Probes. For Ringer solution and ICB, calculations of free and bound concentrations of Ca^{2+}, Zn^{2+}, TPEN, and EGTA were performed with the internet-based WEBMAXSTANDARD program (http://www.stanford.edu/%7Ecpatton/webmaxcE.htm).

Data summary and statistical analysis. Fluorescence intensities were monitored at 10-s intervals throughout each experiment. At discrete time intervals, measurements were summarized as means ± SE. For comparison between treatments, unless stated otherwise, measurements in different regions of interest (6–10 cells for each gland) were combined to provide a single integrated value at each time point for each gland. Unless stated otherwise, comparisons were performed by analysis of variance (ANOVA) for sequential measurements performed with purchased software (Sigma Stat, version 2.0, Jandel).

RESULTS

Measurements of $[Ca^{2+}]_i$ in gastric with fura-2: calibration and control for contributions of heavy metal polyvalent cations. Previous reports have demonstrated the feasibility of using dyes such as fura-2 or fluo-3 to monitor $[Ca^{2+}]_i$ in gastric parietal cells in response to physiological stimuli (9, 41). These approaches depend on assumptions (41) that have not been fully tested under conditions in which glands might be exposed to oxidants or other potentially cytotoxic agents. One assumption is that the dye is concentrated in the cytoplasm. To confirm loading of dye in the cytoplasm, glands loaded with fura-2 AM were monitored during excitation at 340 and 380 nm. As has been noted previously (41), these cells are easily distinguished from chief cells and other cell types by their characteristic large size and bulging basolateral surface, often associated with a conical configuration (Fig. 1), before and after exposure of glands to 10 μM digitonin, an agent that permeabilizes the cell membrane without disturbing transport of secretory function of intracellular organelles (8, 28, 31). In five separate experi-

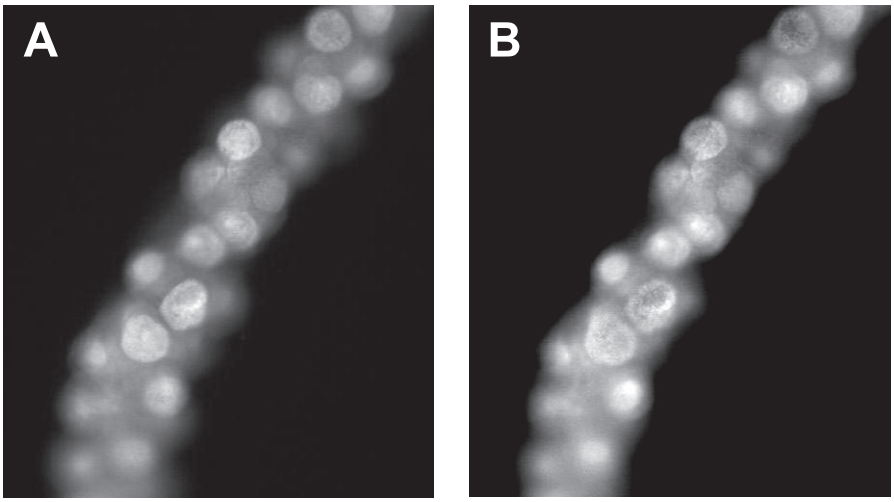

Fig. 1. Digital images in gray scale of an isolated rabbit gastric gland loaded with fura-2 AM (8 μM) for 25 min. *A*: fluorescence excitation at 340 nm when perfused with Ringer solution. *B*: fluorescence excitation when perfused with Ringer solution containing free *N,N,N′,N′*-tetrakis-(2-pyridylmethyl)ethylenediamine (TPEN) ~20 μM. Original magnification ×30.

ments, exposure to digitonin markedly decreased fluorescence at both wavelengths by 85–90% (data not shown), indicating that the dominant contribution to fluorescence signals comes from the cytoplasm.

A second assumption is that contributions of interfering cations are not detected by the fluorescent reporter. We performed two sets of studies to explore the potential influence of heavy metal cations on fura-2 fluorescence in gastric parietal cells. First, we determined the apparent K_d of fura-2 for Zn^{2+} within the parietal cell of the gastric gland. Gastric glands loaded with fura-2 AM were perfused with Ringer solutions containing a strong chelator (0.3 mM EGTA) and no added Ca^{2+}. The glands were then exposed to solutions containing the Zn^{2+} ionophore pyrithione (50 μM) and progressively higher [Zn^{2+}] (0.25, 2.5, 5.0, 7.5, 10, and 25 nM). As shown in a typical recording (Fig. 2), the dye is responsive over the range of 0.25–10 nM. In five glands (n = 32 cells) we determined that the apparent K_d of fura-2 for Zn^{2+} is 2.9 ± 0.3 nM in the parietal cell. These findings indicate that physiologically and pathologically relevant increases of $[Zn^{2+}]_i$ in the nanomolar range may well be reported by fura-2.

In the second set of studies, we explored the feasibility of using the heavy metal chelator TPEN to buffer against increases in heavy metals without compromising the quality of the calcium signals. This heavy metal chelator has very high affinity for non-Ca^{2+} heavy metals such as Zn^{2+} and Fe^{2+} (~10^{-15} M) (2) and low affinity for Ca^{2+} (K_d ~100 μM) (2, 8). Thus exposure to TPEN in the range of 10–20 μM would screen out contributions of interfering metal cations while permitting fura-2 to respond to physiological levels of Ca^{2+} accumulation in the cytoplasm (100 nM to 10 μM) (30). As shown in Fig. 1 the presence of 20 μM TPEN alters baseline patterns of fura-2 fluorescence minimally or not at all.

Initially, we determined the apparent K_d of fura-2 for Ca^{2+} when loaded in the parietal cell. As above, gastric glands loaded with fura-2 AM were perfused with Ringer solutions containing a strong chelator (0.3 mM EGTA) and no added Ca^{2+}. The glands were then exposed to solutions containing the Ca^{2+} ionophore ionomycin and TPEN (20 μM); after equilibration with ionomycin glands were exposed to progressively higher [Ca^{2+}] (100 nM to 20 μM). As shown in Fig. 3 exposure of glands to incremental increases in [Ca^{2+}] in the

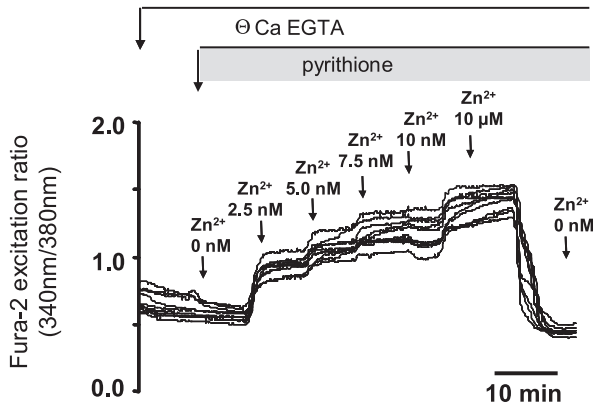

Fig. 2. Fura-2 signals in isolated rabbit gastric glands during incremental increases in Zn^{2+} concentration ([Zn^{2+}]). Glands were exposed initially to Ca^{2+}-depleted Ringer solution (no added Ca^{2+}, 0.5 mM EGTA) and then to EGTA/Ringer with [Zn^{2+}] varying from 2.5 nM to 10 μM, in the presence of pyrithione (50 μM). From averaged values for 4 glands, the K_d of fura-2 for Ca^{2+} is 2.9 ± 0.3 nM.

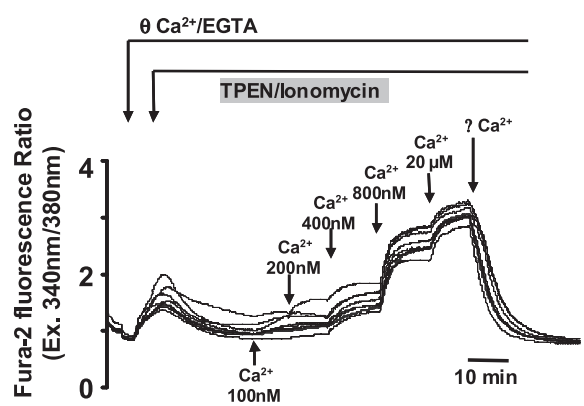

Fig. 3. Fura-2 signals in isolated rabbit gastric glands during incremental increases in Ca^{2+} concentration ([Ca^{2+}]). Glands were exposed initially to Ca^{2+}-depleted Ringer solution (no added Ca^{2+}, 0.5 mM EGTA) and then to EGTA/Ringer with [Ca^{2+}] varying from 100 to 800 nM, in the presence of ionomycin (10 μM) and TPEN (20 μM). From averaged values for 8 glands, the K_d of fura-2 for Ca^{2+} is 380 ± 35 nM.

presence of ionomycin and TPEN disclosed incremental and reversible increases in the excitation ratio, thereby permitting direct correlation of fura-2 signals to $[Ca^{2+}]$. Under these conditions, we calculate that the apparent K_d of fura-2 for Ca^{2+} is 380 ± 35 nM (mean ± SE; n = 49 cells in 9 glands). This value is higher than that reported in cultured cells (22, 26) but close to that reported previously for parietal cells in gastric glands (41). Based on a log-linear plot of fluorescence vs. concentration, baseline levels of $[Ca^{2+}]_i$ in Ringer-perfused glands are ~160 nM.

We also evaluated whether the presence of TPEN would interfere with the ability of fura-2 to monitor Ca^{2+} accumulation in the cytoplasm in the parietal cell during maneuvers known to release Ca^{2+} from intracellular stores. In one set of studies, glands were exposed to ionomycin (10 μM) and nigericin (7 μM) together, maneuvers that not only optimize release of Ca^{2+} but also may release loosely bound heavy metal cations from acidic as well as nonacidic intracellular stores (16, 23, 46). In seven individual gland experiments (Fig. 4), exposure to ionomycin and nigericin increased the fluorescence excitation ratio (340/380 nm), indicating release of Ca^{2+}. The experiments were also performed when glands were preperfused with Ca^{2+}-depleted Ringer containing 20 μM TPEN, a level sufficient to bind heavy metals accumulating in the low micromolar range (2). Comparing outcomes (peak effects) in studies performed in the presence or absence of TPEN (Fig. 4, *bottom*), it appears that the presence of TPEN did not substantially alter the fluorescence excitation ratio (340/380 nm) at baseline or during exposure to ionomycin/nigericin.

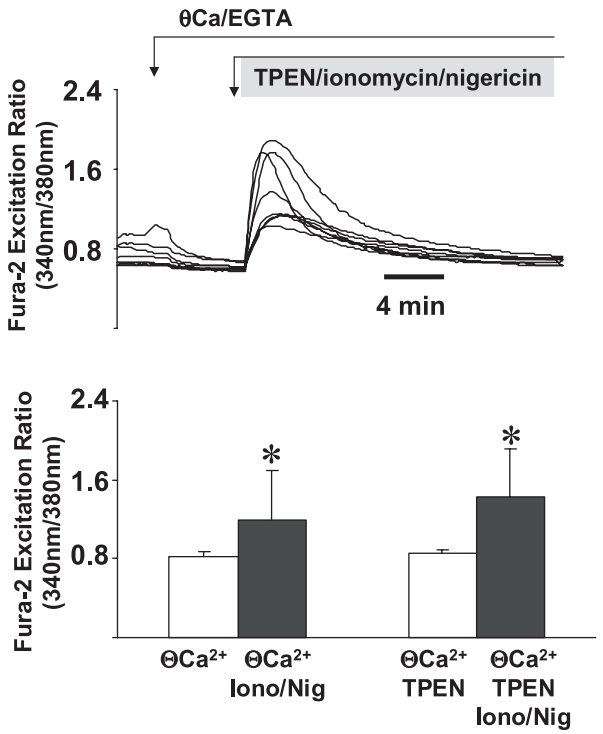

Fig. 4. Summary of measurements of fura-2 fluorescence during release of Ca^{2+} and other metals during exposure to ionomycin (10 μM) and nigericin (7 μM) alone or in the presence of the heavy metal chelator TPEN. *Top*: individual recording showing responses of 7 parietal cells in a single gastric gland. *Bottom*: summary of peak responses in glands exposed to ionomycin/nigericin in the presence or absence of TPEN (n = 7/group). Results are means ± SE. *$P < 0.0001$, comparing measurements before and at the peak response to ionomycin/nigericin (paired t-test).

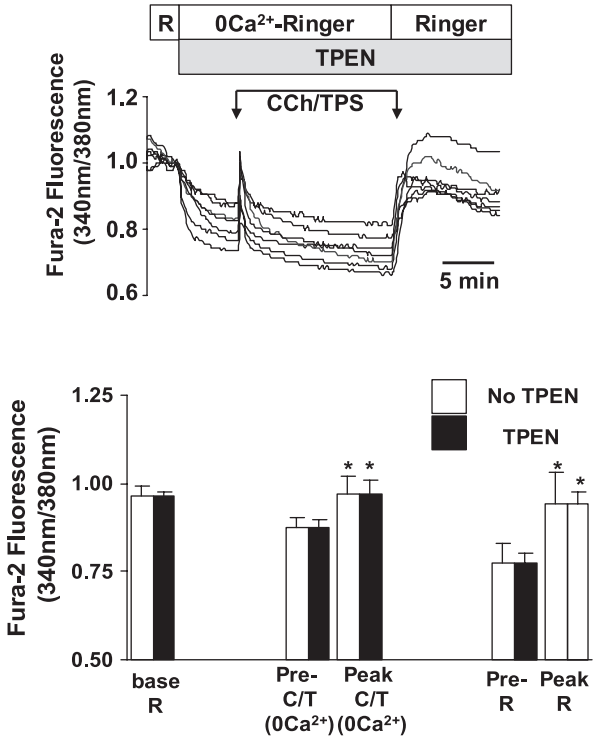

Fig. 5. Effect of TPEN on "pure" intracellular Ca^{2+} signals monitored by fura-2. *Top*: individual experiment, each line representing a recording from an individual parietal cell. The recordings begin when the gland is exposed to Ringer solutions containing no added Ca^{2+}, 0.5 mM EGTA and TPEN (20 μM). The presence of TPEN had no effect on signals generated during exposure to 100 μM carbachol (CCh) and 2 μM thapsigargin (TPS). Also, TPEN had no effect on signals when extracellular Ca^{2+} (1 mM) was restored. *Bottom*: summary of changes in fura-2 signals under control conditions (n = 7) or in the presence of TPEN (n = 6). *Differences between "pre" and "peak" signals are significant ($P < 0.01$) within each group, but not between the 2 groups of glands. base R, baseline Ringer solution; C/T, carbachol/thapsigargin; pre-R, prerestoration of Ringer solution; peak R, peak after restoration of Ringer solution.

We then determined whether TPEN would interfere with the ability of fura-2 to measure physiological increases in $[Ca^{2+}]$. Glands were perfused with Ringer solutions under control conditions and then during exposure to a combination of carbachol and thapsigargin. These agents cause release of Ca^{2+} from intracellular stores and prevent reuptake, thereby maximizing accumulation in the cytoplasm (30–32). In addition, irreversible release of intracellular stores activates capacitative entry of Ca^{2+} from the extracellular spaces to the cytoplasm, increasing the magnitude of Ca^{2+} accumulation (43). Studies were thus performed under control conditions and during exposure to solutions in which total Ca^{2+} and total TPEN were calculated to maintain $[Ca^{2+}]$ at 1 mM and free TPEN at ~20 μM (assuming K_d of TPEN for Ca^{2+} of ~60–100 μM, total Ca^{2+} 1.2 mM, total TPEN 220 μM). As shown in Fig. 5, the presence of TPEN did not alter $[Ca^{2+}]$ signals elicited by carbachol/thapsigargin or during reentry from the extracellular fluid. These studies confirm that TPEN screens out contributions of heavy metals but does not interfere with the ability of fura-2 to monitor accumulation of Ca^{2+} in the cytoplasm.

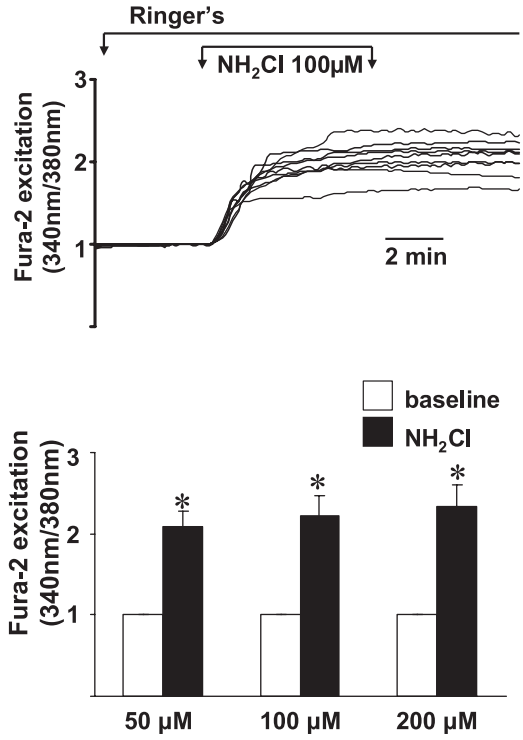

Fig. 6. Measurements of fura-2 signals during exposure of gastric glands to NH_2Cl. *Top*: recordings from individual parietal cells ($n = 7$) in an individual gland exposed to 100 μM NH_2Cl. Recording begins with the gland perfused by standard Ringer solution, then exposure to NH_2Cl, and then standard Ringer solution. Note absence of reversibility. *Bottom*: summary of responses (steady-state response after 12 min) to NH_2Cl at different doses (50, 100, and 200 μM; $n = 5$ experiments at each concentration). All experiments were performed with the protocol outlined at *top*. Results are means ± SE of responses of individual glands.*$P < 0.001$ compared with baseline (ANOVA).

Responses of fura-2-loaded gastric glands to NH_2Cl. Previously we noted (10) that NH_2Cl remained stable for 6 h in Ringer solution with <10% loss of absorbance at 242 nm. All experiments were conducted within this interval after preparation of NH_2Cl. In initial experiments, fura-2 responses were monitored during exposure of isolated gastric glands to Ringer solutions with [NH_2Cl] of 50, 100, or 200 μM. Initially, exposure to NH_2Cl led to a marked increase, then a more prolonged and gradual increase in the fluorescence excitation ratio 340/380 nm (Fig. 6, *top*). These signals were not reversed when the oxidant was removed. Curiously (Fig. 6, *bottom*), minimal differences were observed in responses to increasing [NH_2Cl] over the range tested.

Control studies were performed to evaluate the specificity of the responses to NH_2Cl. Similar effects were not observed when glands ($n = 3$ in each group) were exposed to NH_4Cl (20 mM), HOCl (200 μM), H_2O_2 (200 μM) or the membrane-impermeant compound TaurNHCl. These findings indicate that responses are confined to membrane-permeant choramine species.

Contributions of intracellular stores of Ca^{2+} in response to NH_2Cl. In other cell types, heavy metal cations such as Zn^{2+} have been shown to contribute significantly to the fura-2 signal observed during exposure to NH_2Cl (10). We performed studies to monitor the effects of NH_2Cl on release of Ca^{2+} from intracellular sources in the absence of interfering metal cations. Isolated fura-2-loaded gastric glands were perfused with Ca^{2+}-free Ringer solution containing EGTA (0.5 mM) and TPEN (20 μM). Responses were then monitored before, during, and after NH_2Cl was present at a concentration of 50, 100, or 200 μM. When glands are perfused under these conditions, the excitation ratio decreases markedly (Fig. 7), corresponding to levels of [Ca^{2+}] of 10 nM or lower. Starting at this baseline, NH_2Cl elicits dose-dependent, modest, and nonreversible increases in $[Ca^{2+}]_i$. With the calibrations in Fig. 3 as a reference, exposure to 200 μM NH_2Cl increases $[Ca^{2+}]_i$ to levels between 200 and 300 nM above the baseline.

To more conclusively evaluate effects of NH_2Cl on emptying and filling of intracellular stores, we performed studies in isolated rabbit gastric glands loaded with mag-fura-2 AM. This low-affinity, Ca^{2+}-sensitive reporter (K_d ~100 μM) has been used to monitor [Ca^{2+}] in subcellular compartments of the gastric gland after permeabilization to eliminate dye in the cytoplasm (31, 32). At baseline, the dominant portion of the signal was attributable to the high content of Ca^{2+} in the endoplasmic reticulum (31, 32). The very low affinity of mag-fura-2 for Mg^{2+} (K_d ~1.5 mM) makes it very unlikely that Mg^{2+} contributes to mag-fura-2 fluorescence in a store that has a high content of Ca^{2+}, for which mag-fura-2 has a much higher affinity (K_d ~100 μM) (26). Moreover, studies in this same preparation of the isolated rabbit gastric gland (31, 32), and in other cell types and species (18), also excluded a significant contribution of Mg^{2+} to mag-fura-2 fluorescence in permeabilized preparations.

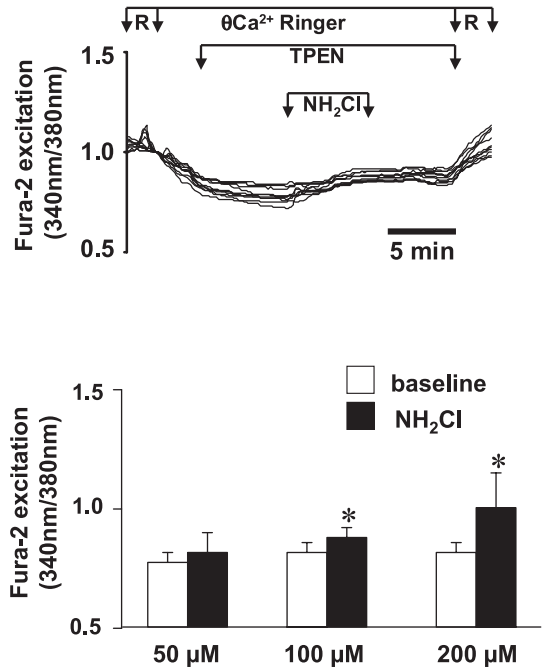

Fig. 7. *Top*: Recordings from individual parietal cells ($n = 8$) in an individual gland exposed to 100 μM NH_2Cl in the presence of TPEN (20 μM). Recording begins with the gland perfused by standard Ringer solution (R), then switch to calcium-depleted Ringer solution, and then exposure to NH_2Cl and then standard Ringer solution. Note absence of reversibility. *Bottom*: averaged responses to NH_2Cl at different doses (50, 100, and 200 μM). Each bar represents responses in 4 or 5 separate experiments ($n = 6$–9 parietal cells/gland), each conducted in exactly the same sequence as described at *top*. Results are means ± SE, with *y*-axis indicating excitation ratio (340/380 nm). *$P < 0.01$ compared with baseline by ANOVA.

However, mag-fura-2 also has a much higher affinity for heavy metals such as Zn^{2+} (K_d ~3 nM) (26). To eliminate contributions of heavy metals, studies were again performed in the presence of TPEN at a concentration (10 μM) high enough to chelate heavy metal components but not so high as to alter Ca^{2+} content in highly concentrated intracellular stores (6, 30). In six permeabilized glands loaded with mag-fura-2 AM, exposure to 10 μM TPEN alone modestly increased (<10% above baseline) the fluorescence excitation ratio (340/380 nm), indicating that intracellular stores monitored by mag-fura-2 may contain small amounts of interfering non-Ca^{2+} metal cations that quench the signal. Further increases were not observed when TPEN concentration was increased to 20 μM ($n = 3$; data not shown). An additional maneuver to confirm that mag-fura-2 reports Ca^{2+} in the high-content store was to expose permeabilized glands to thapsigargin, which inhibits SERCA, thereby preventing Ca^{2+} reuptake into the high-content store. As reported by Hofer and Machen (31, 32), the store monitored by mag-fura-2 was depleted by application of 2 μM thapsigargin ($n = 3$).

To evaluate the effects of NH_2Cl on intracellular stores of Ca^{2+}, we exposed digitonin-permeabilized gastric glands loaded with mag-fura-2 to solutions containing 20 μM TPEN and 100 μM NH_2Cl. As shown in Fig. 8, rapid decreases in the excitation ratio were observed, demonstrating that exposure to NH_2Cl causes a marked depletion of intracellular pools of Ca^{2+} within the parietal cell. Similar responses were observed in six other glands, confirming a nonreversible depletion of intracellular Ca^{2+} stores in response to NH_2Cl, 68 ± 4% compared with baseline ($P < 0.001$).

Contributions of extracellular Ca^{2+}. We next evaluated the effects of NH_2Cl on influx of extracellular Ca^{2+} to the cytoplasm. As noted above, removal of Ca^{2+} from perfusates leads to significant depletion of Ca^{2+} in the cytoplasm, indicating influx from extracellular sources under resting conditions. Two sets of studies were performed to evaluate whether exposure to NH_2Cl accelerates Ca^{2+} influx. In the first set, we compared

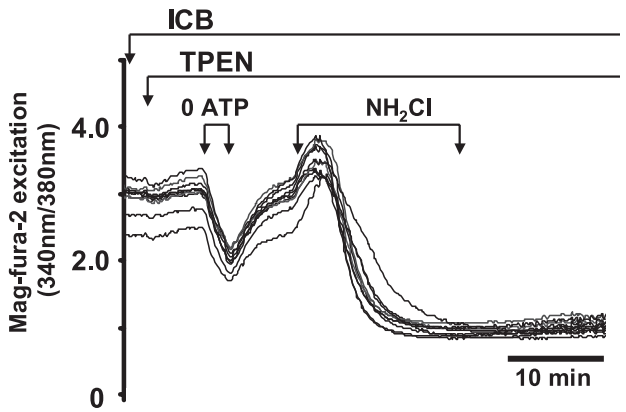

Fig. 8. Mag-fura-2 signals during exposure of an isolated, permeabilized gastric gland to NH_2Cl in the presence of TPEN. Mag-fura-2-loaded glands were permeabilized with α-toxin and then mounted on a coverslip for fluorescence imaging at 520 nm (alternating excitation at 340 and 380 nm). Each line represents a recording of mag-fura-2 responses in an individual parietal cell. Recording begins as gland is perfused with intracellular buffer (ICB; 0.5 mM ATP) and then exposed to TPEN (20 μM). A brief removal and repletion of ATP from the perfusate confirms that the gland is permeabilized. Exposure to 100 μM NH_2Cl demonstrates complete and nonreversible emptying of intracellular stores.

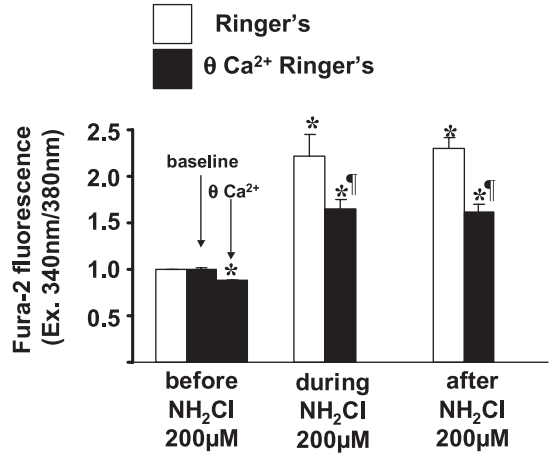

Fig. 9. Comparison of responses to NH_2Cl in the presence or absence of extracellular Ca^{2+}. Each column represents integrated response (mean ± SE) of 6 glands (6–8 cells/gland) when a stable baseline was achieved after the change in experimental condition. *$P < 0.05$ compared with Ringer solution baseline (ANOVA); ¶$P < 0.05$ compared with baseline or Ringer solution control.

responses to NH_2Cl in Ringer solution or to NH_2Cl in Ca^{2+}-free Ringer solutions. In these studies, TPEN was not included, so as not to create undue disturbances by the exclusion of heavy metals. As summarized in Fig. 9, increases in excitation ratio were significantly lower ($P < 0.01$) when glands were exposed to 200 μM NH_2Cl in the absence of extracellular Ca^{2+}. These experiments confirm that extracellular Ca^{2+} plays a significant role in the overall response to NH_2Cl.

We then performed studies to more precisely evaluate whether influx of Ca^{2+} is accelerated during the exposure to NH_2Cl. The strategy in these studies was to observe Ca^{2+} influx after depletion and then restoration of extracellular Ca^{2+}, after exposure to NH_2Cl. After equilibration with Ringer solutions, two groups of glands were perfused for 5–7 min with Ca^{2+}-free Ringer solution containing 20 μM TPEN. The control group was perfused for an additional 5–7 min with Ca^{2+}-free/TPEN solutions, while the other group was perfused with Ca^{2+}-free/TPEN containing 200 μM NH_2Cl. Both groups were then perfused with standard 1 mM Ca^{2+}-Ringer solutions containing total Ca^{2+} (1.2 mM) and total TPEN (220 μM) sufficient to maintain free levels of TPEN at ~20 μM. As shown in Fig. 10, removal of extracellular Ca^{2+} in the presence of TPEN elicited significant and comparable decreases in $[Ca^{2+}]_i$ in both groups of glands. As noted above (Fig. 7), exposure to NH_2Cl elicited a modest increase in $[Ca^{2+}]_i$ due to release of intracellular stores. When extracellular Ca^{2+} was restored, increases in $[Ca^{2+}]_i$ were observed in both groups. The magnitude of the recovery in the NH_2Cl group was significantly higher than in the control group, arguing that exposure to NH_2Cl accelerates Ca^{2+} influx above baseline levels.

To provide additional evidence that this accelerated entry from the outside might be due to store-operated entry, influx of Ca^{2+} during the restoration of extracellular Ca^{2+} was monitored after exposure to NH_2Cl. Studies were performed under control conditions or in the presence of 2-aminoethoxydiphenyl borate (2-APB), which has been shown to block store-operated influx of Ca^{2+} in other cell types (5). As shown in

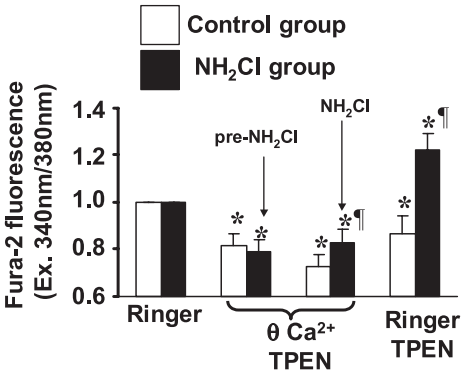

Fig. 10. Influx of extracellular Ca^{2+} after exposure to NH_2Cl. Both groups of glands (control and NH_2Cl) were initially perfused with Ca^{2+}-free Ringer/TPEN for 5 min, then with Ca^{2+}-free/TPEN alone or Ca^{2+}-free/ TPEN + NH_2Cl for 5 min, and then with Ringer/TPEN for 20 min. Because Ringer solution contains 1 mM Ca^{2+}, TPEN concentration was adjusted so that free [TPEN] was ~20 μM. Each column represents integrated response (mean ± SE) of 6 glands (6–8 cells/gland). *$P < 0.05$ compared with Ringer solution baseline (ANOVA); ¶$P < 0.05$ compared with control.

Fig. 11, 2-APB was added to the perfusate after exposure to 100 μM NH_2Cl and just before restoration. In a set of four paired experiments, glands from the same harvest were studied sequentially to minimize variation in responses to NH_2Cl. During the Ca^{2+} restoration phase (after exposure to NH_2Cl), the increase in fluorescence excitation ratio was significantly reduced in the presence of 2-APB (Δ15 min after restoration: 0.17 ± 0.03 arbitrary units) compared with that in its absence (0.34 ± 0.06; $P < 0.05$, ANOVA multiple comparisons). In control studies conducted in the absence of NH_2Cl, responses to removal and restoration of extracellular Ca^{2+} were not altered in the presence of 2-APB (data not shown). Thus it appears that a component of NH_2Cl-induced influx of Ca^{2+} is attributable to store-operated entry.

NH_2Cl-induced Ca^{2+} signals in presence of antioxidants. To determine whether pretreatment with antioxidants would prevent responses, glands loaded with fura-2 were perfused with Ringer solutions containing antioxidants (1 mM VitC, 100 μM DTT, or 1 mM DTT) before exposure to NH_2Cl. With each antioxidant ($n = 4$ or 5 glands), pretreatment for 4–8 min prevented any response to NH_2Cl at concentrations up to 200 μM (data not shown).

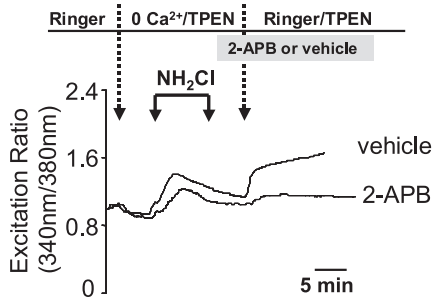

Fig. 11. Effects of 2-aminoethoxydiphenyl borate (2-APB) on store-operated entry induced by NH_2Cl. Superimposed recordings from fura-2-loaded glands from the same harvest are shown. Both glands were exposed to 100 μM NH_2Cl in a protocol similar to that in Fig. 9, with similar responses. As before, 20 μM TPEN was present to screen out contributions from heavy metal cations. After removal of NH_2Cl, glands were exposed to 2-APB or vehicle (ethanol 1:1,000), and then extracellular Ca^{2+} was restored.

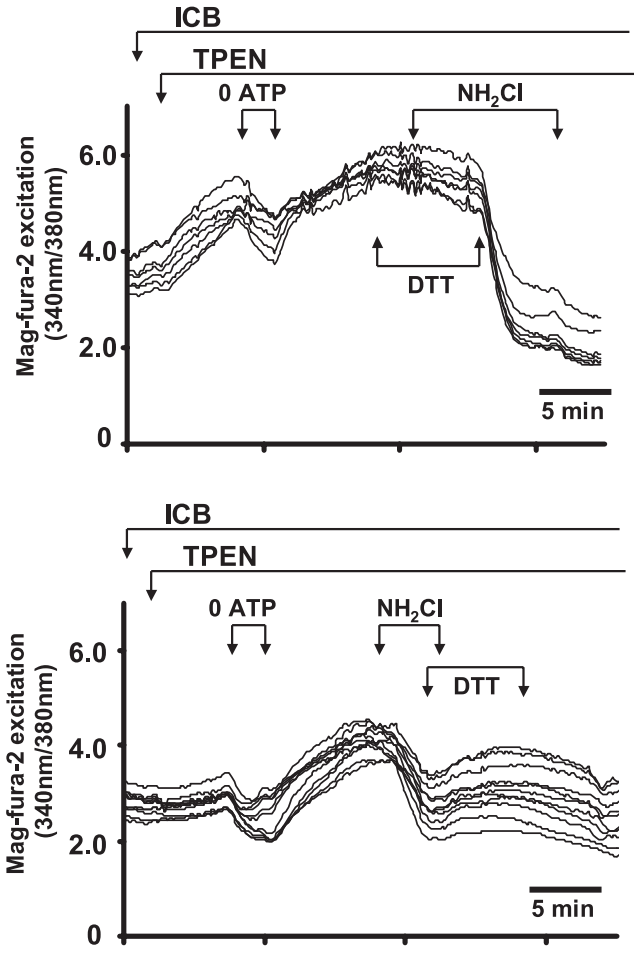

Fig. 12. Thiol reduction as a means of preventing or reversing NH_2Cl effects on intracellular Ca^{2+} stores. Glands loaded with mag-fura-2 were permeabilized with *Staphylococcus aureus*α-toxin in ICB and then mounted on the microscope stage. Before exposure to NH_2Cl, each gland was perfused with ICB from which ATP was removed, to confirm successful permeabilization. *Top*: recording in an individual gland exposed to NH_2Cl in ICB already containing 1 mM dithiothreitol (DTT). DTT is then removed, with NH_2Cl remaining present, thereby allowing stores to empty. *Bottom*: recording in an individual gland exposed to 1 mM DTT after initiation of responses to 100 μM NH_2Cl. NH_2Cl is then removed, with DTT remaining, thereby arresting and partially reversing effects of NH_2Cl. In both panels, individual lines represent recordings from individual parietal cells.

Of greater interest was whether responses might be arrested and reversed if the antioxidant were administered during ongoing exposure to NH_2Cl. To characterize the influence of different antioxidants on Ca^{2+} release and filling of intracellular stores, glands were loaded with mag-fura-2 AM, permeabilized with α-toxin, and equilibrated with TPEN-containing intracellular buffer. As shown in Fig. 12, *top*, exposure to DTT before application of 200 μM NH_2Cl prevents depletion of the stores. Moreover, after NH_2Cl has been added, application of DTT arrests and partially reverses the precipitous decrease in store content (Fig. 12, *bottom*). In contrast, pretreatment with VitC prevented emptying of stores during subsequent exposure to NH_2Cl. However, application of VitC after exposure to NH_2Cl did not lead to any reversal of store depletion ($n = 4$ individual glands in separate experiments; data not shown).

We then performed studies to provide insight into the effects of different antioxidants during NH_2Cl-induced accumulation

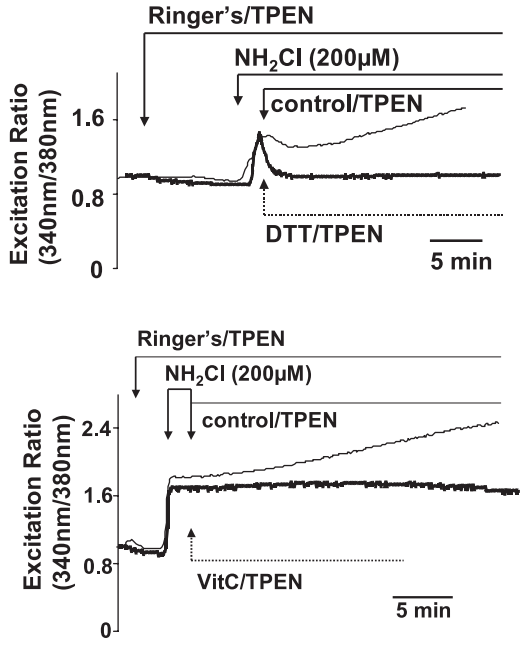

Fig. 13. Effectiveness of different antioxidants in reversing NH_2Cl-induced accumulation of Ca^{2+} in the cytoplasm. Before exposure to NH_2Cl, each gland was perfused with Ringer solution containing a sufficient amount of TPEN (0.2 mM) and Ca^{2+} (1.2 mM) to maintain free [TPEN] at ~20–50 μM. *Top*: recording in individual glands (from same harvest) exposed to NH_2Cl in the presence or absence of the thiol-reducing agent DTT. Thin line represents summary of 8 parietal cells in an individual gland exposed to NH_2Cl alone; thick line represents summary of 7 parietal cells in an individual gland exposed to NH_2Cl and DTT. *Bottom*: recording in individual glands (from same harvest) exposed to NH_2Cl in the presence or absence of the oxidant scavenger vitamin C (VitC). Thin line represents summary of 8 parietal cells in an individual gland exposed to NH_2Cl alone; thick line represents summary of 8 parietal cells in an individual gland exposed to NH_2Cl and VitC.

of Ca^{2+} in the cytoplasm of the parietal cell. Glands were loaded with fura-2 AM, equilibrated with Ringer solution containing total TPEN (220 μM) and Ca^{2+} (1.2 mM) to maintain free [TPEN] at 20–50 μM, and then exposed to NH_2Cl (200 μM). In earlier studies (10), we observed that addition of DTT (up to 1 mM) does not destabilize or deplete NH_2Cl levels in the Ringer solution. Thus it was possible to observe the effects of DTT in the presence of an ongoing exposure to NH_2Cl. As shown in Fig. 13, *top*, addition of 1 mM DTT to the perfusate at the peak of the NH_2Cl effect led to a rapid decrease in $[Ca^{2+}]_i$, consistent with the previous observation that addition of DTT would reverse NH_2Cl-induced depletion of intracellular Ca^{2+} stores (Fig. 12) and suggesting, in addition, that store-operated entry of extracellular Ca^{2+} is also reversed. The rate of reversal was measured as the decline from peak value at 1 min. This rate was significantly accelerated after addition of DTT ($P < 0.01$): 43.2 ± 6.5% ($n = 8$ glands) compared with 9.1 ± 1.9% ($n = 10$ glands) after simple exchange of the perfusing Ringer solution.

In contrast, we observed that addition of 1 mM VitC consumed NH_2Cl in Ringer solutions, as monitored by a complete loss of absorbance at 242 nm. Thus it was not feasible to observe the effects of VitC while maintaining a steady level of NH_2Cl in the perfusate. In studies of this antioxidant, glands were exposed briefly to Ringer solution containing NH_2Cl (200 μM) and then to Ringer solution or Ringer solution containing VitC (1 mM). As shown in Fig. 13, *bottom*, introduction of VitC did not reverse the effects of NH_2Cl. In the presence of VitC ($n = 7$), we never observed a continued accumulation of Ca^{2+} in the cytoplasm that was occasionally present in control glands (3 of 7) after removal of NH_2Cl.

Finally, we performed Western blots to evaluate effects of NH_2Cl on expression of Ca^{2+} transport proteins. We used an antibody directed at SERCA2, which is responsible for store refilling (7) and is expressed in gastric mucosa (39). In addition, we utilized an antibody directed at the plasma membrane NCX, which has been implicated in disposal of cytoplasmic Ca^{2+} and isoforms of which have been identified in intestinal epithelia (15). As shown in Fig. 14, *top*, incubation of gastric glands for 1 h with NH_2Cl (100 μM) almost completely depleted expression of the SERCA2 isoform at its characteristic ~110-kDa position, an effect prevented by pretreatment with 1 mM DTT. Other, nonspecific bands were also detected and were not responsive to NH_2Cl or rescue with DTT. Similarly, the characteristic bands (15) for NCX (120 and 70 kDa) were depleted in response to NH_2Cl and protected when DTT was present. Additional control studies (not shown) demonstrated that pretreatment with DTT, in the absence of NH_2Cl, had no effect on expression of SERCA2 or NCX. Moreover, we found that NH_2Cl had no effect on expression on expression of the α-subunit of the Na^+-K^+-ATPase, indicating that the effects of NH_2Cl are not attributable to nonspecific destruction of transporter proteins.

DISCUSSION

Considerable experimental evidence indicates that NH_2Cl is likely to be present in gastric mucosa during acute *H. pylori*-induced gastritis. When luminal solutions contain relevant concentrations of NH_3, mucosal injury is amplified under conditions that activate neutrophils (12, 50). In addition, strategies aimed at neutralizing chloramines appear to attenuate mucosal injury caused by *Helicobacter* infestation (33). Accu-

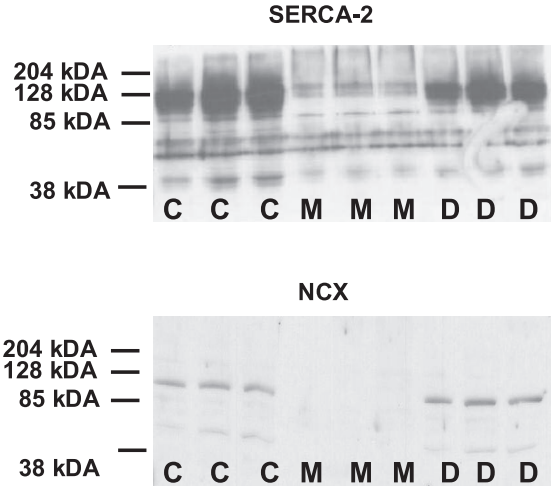

Fig. 14. Alterations in Ca^{2+} transporter expression during exposure to NH_2Cl. Western blots utilizing antibodies reacting with sarco(endo)plasmic reticulum Ca^{2+}-ATPase (SERCA; *top*) isoform 2 and with known isoforms for Na^+/Ca^{2+} exchangers (NCX; *bottom*) are shown. *Lanes C*, control glands incubated in Ringer solution for 1 h; *lanes M*, gland preparations incubated for 1 h in the presence of 100 μM NH_2Cl; *lanes D*, glands incubated for 1 h with both NH_2Cl (100 μM) and DTT (1 mM).

mulation of NH_2Cl is not unique to the gastric mucosa: it can occur in colon and other organs where activated neutrophils come into contact with NH_3 generated from bacterial or host metabolism (20, 21, 24, 52). Thus the effects of chloramines on cell signaling pathways are of interest in cell systems potentially susceptible to different forms of oxidative and nitrosative stress.

Our studies indicate that, at pathologically relevant concentrations (20, 21, 24, 52), exposure to NH_2Cl causes accumulation of free Ca^{2+} in the cytoplasm of the gastric parietal cell. Accumulation of Ca^{2+} results from emptying of intracellular stores and from the ensuing activation of store-operated entry from the extracellular spaces. In addition, the effects of NH_2Cl on expression of SERCA2 and NCX argue that an additional effect of NH_2Cl is to impair mechanisms that dispose of Ca^{2+} loading in the cytoplasm. These effects are not duplicated by precursor oxidants, such as peroxide or HOCl, nor are they elicited by membrane-impermeant chloramines such as taurochloramine. Thus the effects of NH_2Cl on Ca^{2+} mobilization and accumulation in the cytoplasm appear to be specific to the chloramine moiety. These effects are neutralized by concurrent exposure to oxidant scavengers such as VitC; moreover, they can be prevented, arrested, and at least partly reversed by exposure to thiol-reducing agents such as DTT. This latter observation provides evidence that at least some substantial component of NH_2Cl-induced accumulation of Ca^{2+} is the result of a targeted and reversible oxidative process, and not an irreversible leakage of Ca^{2+} from injured compartments and cells. To our knowledge, these studies are the first to examine the effects of thiol oxidants on intracellular Ca^{2+} homeostasis in gastric epithelial cells in a primary cell preparation, the gastric gland. In addition, these are the first studies to directly evaluate the effects of pathologically relevant thiol-directed oxidants and reducing agents on release of Ca^{2+} from intracellular stores in any primary epithelial cell preparation, either functionally or at the molecular level.

These studies raise three issues for discussion. The first issue involves the mechanisms by which NH_2Cl causes accumulation of Ca^{2+} within the cytoplasm of the gastric parietal cell. With respect to $[Ca^{2+}]_i$, our studies indicate that NH_2Cl-induced increases are due in part to release from intracellular stores. The comparison of responses to perfusates with and without Ca^{2+} makes it clear that entry of extracellular Ca^{2+} is also responsible for a major component of the NH_2Cl-induced signal. These responses are attributable to thiol modification of Ca^{2+} transport processes, since DTT prevented and reversed effects of NH_2Cl on fura-2 signals. Entry of extracellular Ca^{2+} might be due to influx through capacitative entry, activated when carbachol- and thapsigargin-sensitive stores are released (30–32). Consistent with this explanation is our observation that 2-APB at least partially inhibits influx of NH_2Cl-induced extracellular Ca^{2+}. Further studies would be required to address the possibility that disposal of accumulating Ca^{2+} is also impaired by exposure to thiol-directed oxidants. Specific mechanisms to be studied would include the capacity of the mitochondrion to buffer the cytoplasm against increases in $[Ca^{2+}]_i$ (45) and clearance of Ca^{2+} in the cytoplasm through membrane extrusion processes, such as the plasma membrane Ca^{2+}-ATPase (PMCA) (7).

The second issue raised by our studies involves the consequences of oxidant-induced increases in $[Ca^{2+}]_i$ and $[Zn^{2+}]_i$ in the gastric gland. In diverse in vitro cell culture models, agonist-stimulated increases in $[Ca^{2+}]_i$ enhance mitochondrial respiration and substrate utilization (34, 45). In excess, increases in $[Ca^{2+}]_i$ induce mitochondrial depolarization and the initiating events of apoptosis and/or cell necrosis (42). However, the effects of more limited and controlled oxidant-induced increases in $[Ca^{2+}]_i$, such as those reported here, have not been characterized. Indirect evidence suggests that such limited increases in $[Ca^{2+}]_i$ oppose the generally suppressive effects of the increases in $[Zn^{2+}]$ induced by NH_2Cl (Dubach JM, Naik HB, Beshire MA, Wieland AM, Walsh BM, Soybel DI, unpublished observations). Moreover, they also oppose the generally toxic effects of NH_2Cl-induced accumulation of Zn^{2+} in the cytoplasm. Thiol oxidant-induced alterations in the balance between $[Ca^{2+}]_i$ and $[Zn^{2+}]_i$ may thus prove to be a useful target in modulating injury caused by the inflammatory microenvironment caused by ischemia-reperfusion or infestation with *H. pylori*.

The last issue for discussion is technical, namely, the strengths and limitation of fluorescence methods used to monitor intracellular divalent cation signals. Calcium-sensing fluorescent indicator dyes all are responsive to other polyvalent cations. Potentially interfering polyvalent cations that might be released from intracellular pools include Fe^{2+}, Fe^{3+}, Cu^{2+}, and Zn^{2+}. The most widely used fluorescent reporter, fura-2, is quenched in response to Cu^{2+}, Fe^{2+}, and Fe^{3+}. However, it responds to Zn^{2+} in a manner similar to Ca^{2+}. Previous reports and manufacturer specifications indicate that, in vitro, fura-2 has a higher affinity for Zn^{2+} ($K_d \sim 3$–15 nM) than for Ca^{2+} ($K_d \sim 150$–300 nM) (26, 35, 41). Our calibration studies confirm these ranges of sensitivities to Zn^{2+} and Ca^{2+} in situ in cells of the rabbit gastric gland.

Mag-fura-2 has a much lower affinity for Ca^{2+}, with a reported K_d of 25–60 μM (26), a property that has made it useful for monitoring intracellular stores of Ca^{2+} in the range of 10–100 μM (31, 32). In cell-free solutions, mag-fura-2 has a reported K_d for Zn^{2+} of ~20 nM (13, 26). In situ, however, mag-fura-2 does not respond sensitively to $[Zn^{2+}]$ in the nanomolar range, perhaps because responses to high-concentration, intracellular Ca^{2+} stores are dominant. Our studies send a fundamental message that, in using fluorescent reporters to explore changes in $[Ca^{2+}]_i$ during exposure to oxidants, toxins, and relatively uncharacterized neurohumoral agonists, it is important to take into account accumulation of interfering polyvalent cations.

In summary, we have adapted fluorometric approaches for monitoring changes in $[Ca^{2+}]_i$ in isolated glands of the rabbit gastric mucosa during exposure to oxidant stress. When contributions of interfering metal cations are controlled, it appears that NH_2Cl elicits increases in $[Ca^{2+}]_i$ that are sustained and not necessarily higher than those expected from normal signaling processes. These increases reflect contributions from emptying of physiologically regulated intracellular stores, as well as store-operated entry of extracellular Ca^{2+}. Our studies also indicate that these increases are mediated by oxidation of sulfhydryl (thiol) groups that are probably targeted by other endogenously generated oxidants, for example, nitric oxide. Further studies will determine the role played by Ca^{2+} signaling in the cellular response to thiol oxidants produced during acute tissue injury.

GRANTS

This work was supported by National Institute of Diabetes and Digestive and Kidney Diseases Grant R01-DK-069929 and Brigham Surgical Group Foundation (D. I. Soybel) and by Howard Hughes Medical Institute Student Fellowships (H. B. Naik and A. M. Wieland).

REFERENCES

1. **Andres PG, Friedman LS.** Epidemiology and the natural course of inflammatory bowel disease. *Gastroenterol Clin North Am* 28: 225–281, 1999.
2. **Arslan P, Di Virgilio F, Beltrame M, Tsien RY, Pozzan T.** Cytosolic Ca^{2+} homeostasis in Ehrlich and Yoshida carcinomas. A new, membrane-permeant chelator of heavy metals reveals that these ascites tumor cell lines have normal cytosolic free Ca^{2+}. *J Biol Chem* 260: 2719–2727, 1985.
3. **Banan A, Fields JZ, Zhang Y, Keshavarzian A.** Key role of PKC and Ca^{2+} in EGF protection of microtubules and intestinal barrier against oxidants. *Am J Physiol Gastrointest Liver Physiol* 280: G828–G843, 2001.
4. **Berglindh T, Obrink KJ.** A method for preparing isolated glands from the rabbit gastric mucosa. *Acta Physiol Scand* 96: 150–159, 1976.
5. **Bootman MD, Collins TJ, Mackenzie L, Roderick HL, Berridge MJ, Peppiatt CM.** 2-Aminoethoxydiphenyl borate (2-APB) is a reliable blocker of store-operated Ca^{2+} entry but an inconsistent inhibitor of $InsP_3$-induced Ca^{2+} release. *FASEB J* 16: 1145–1150, 2002.
6. **Caroppo R, Colella M, Colasuonno A, DeLuisi A, Debellis L, Curci S, Hofer AM.** A reassessment of the effects of luminal [Ca^{2+}] on inositol 1,4,5-trisphosphate-induced Ca^{2+} release from internal stores. *J Biol Chem* 278: 39503–39508, 2003.
7. **Caroppo R, Gerbino A, Debellis L, Kifor O, Soybel DI, Brown EM, Hofer AM, Curci S.** Asymmetrical, agonist-induced fluctuations in local extracellular [Ca^{2+}] in intact polarized epithelia. *EMBO J* 20: 6316–6326, 2001.
8. **Caroppo R, Gerbino A, Fistetto G, Colella M, Debellis L, Hofer AM, Curci S.** Extracellular calcium acts as a "third messenger" to regulate enzyme and alkaline secretion. *J Cell Biol* 166: 111–119, 2004.
9. **Cheng I, Qureshi I, Chattopadhyay N, Qureshi A, Butters RR, Hall AE, Cima RR, Rogers KV, Hebert SC, Geibel JP, Brown EM, Soybel DI.** Expression of an extracellular calcium-sensing receptor in rat stomach. *Gastroenterology* 116: 118–126, 1999.
10. **Cima RR, Dubach JM, Wieland AM, Walsh BM, Soybel DI.** Intracellular Ca^{2+} and Zn^{2+} signals during monochloramine-induced oxidative stress in isolated rat colon crypts. *Am J Physiol Gastrointest Liver Physiol* 290: G250–G261, 2006.
11. **Cooper CE, Patel RP, Brookes PS, Darley-Usmar VM.** Nanotransducers in cellular redox signaling: modification of thiols by reactive oxygen and nitrogen species. *Trends Biochem Sci* 117: 489–492, 2002.
12. **Dekigai H, Murakami M, Kita T.** Mechanism of *Helicobacter pylori*-associated gastric mucosal injury. *Dig Dis Sci* 40: 1332–1339, 1995.
13. **Dineley KE, Malaiyandi LM, Reynolds IJ.** A reevaluation of neuronal zinc measurements: artifacts associated with high intracellular dye concentration. *Mol Pharmacol* 62: 618–627, 2002.
14. **Dineley KE, Votyakova TV, Reynolds IJ.** Zinc inhibition of cellular energy production: implications for mitochondria and neurodegeneration. *J Neurochem* 85: 563–570, 2003.
15. **Dong H, Sellers ZM, Smith A, Chow JYC, Barrett KE.** Na^+/Ca^{2+} exchange regulates Ca^{2+}-dependent duodenal mucosal ion transport and HCO_3^- secretion in mice. *Am J Physiol Gastrointest Liver Physiol* 288: G457–G465, 2005.
16. **Erdahl WL, Chapman CJ, Wang E, Taylor RW, Pfeiffer DR.** Ionophore 4-BrA23187 transports Zn^{2+} and Mn^{2+} with high selectivity over Ca^{2+}. *Biochemistry* 35: 13817–13825, 1996.
17. **Ermak G, Davies KJ.** Calcium and oxidative stress: from cell signaling to cell death. *Mol Immunol* 38: 713–721, 2002.
18. **Fowler MR, Cooper GJ, Hunter M.** Regulation and identity of intracellular calcium stores involved in membrane cross talk in the early distal tubule of the frog kidney. *Am J Physiol Renal Physiol* 286: F1219–F1225, 2004.
19. **Gow A, Ischiropoulos H.** NO running on MT: regulation of zinc homeostasis by interaction of nitric oxide with metallothionein. *Am J Physiol Lung Cell Mol Physiol* 282: L183–L184, 2002.
20. **Grisham MB, Gaginella TS, von Ritter C, Tamai H, Be RM, Granger DN.** Effects of neutrophil-derived oxidants on intestinal permeability, electrolyte transport, epithelial cell viability. *Inflammation* 14: 531–542, 1990.
21. **Grisham MB, Jefferson MM.** Chlorination of endogenous amines by isolated neutrophils. *J Biol Chem* 259: 10404–10413, 1984.
22. **Grynkiewicz G, Poenie M, Tsien RY.** A new generation of Ca^{2+} indicators with greatly improved fluorescence properties. *J Biol Chem* 260: 3440–3450, 1985.
23. **Hamidinia SA, Tan B, Erdahl WL, Chapman CJ, Taylor RW, Pfeiffer DR.** The ionophore nigericin transports Pb^{2+} with high activity and selectivity: a comparison to monensin and ionomycin. *Biochemistry* 43: 15956–15965, 2004.
24. **Hampton MB, Kettle AJ, Winderbourn CC.** Inside the neutrophil phagosome: oxidants, myeloperoxidase, and bacterial killing. *Blood* 92: 3007–3017, 1998.
25. **Harford WV, Barnett C, Lee E, Perez-Perez G, Blaser MJ, Peterson WL.** Acute gastritis with hypochlorhydria: report of 35 cases with long term follow up. *Gut* 47: 467–472, 2000.
26. **Haugland RP.** *Molecular Probes Product Information and Catalogue*. Eugene, OR: Molecular Probes, 2003.
27. **Helander HF, Hirschowitz BI.** Quantitative ultrastructural studies on gastric parietal cells. *Gastroenterology* 63: 951–961, 1972.
28. **Hersey SJ, Steiner L.** Acid formation by permeable gastric glands: enhancement by prestimulation. *Am J Physiol Gastrointest Liver Physiol* 248: G561–G568, 1985.
29. **Hiraishi H, Terano A, Sugimoto T, Harada T, Razandi M, Ivy KJ.** Protective role of intracellular superoxide dismutase against extracellular oxidants in cultured rat gastric cells. *J Clin Invest* 93: 331–338, 1994.
30. **Hofer AM, Fasolato C, Pozzan T.** Capacitative Ca^{2+} entry is closely linked to the filling state of internal Ca^{2+} stores: a study using simultaneous measurements of I_{CRAC} and intraluminal [Ca^{2+}]. *J Cell Biol* 140: 325–334, 1998.
31. **Hofer AM, Machen TE.** Direct measurement of free Ca in organelles of gastric epithelial cells. *Am J Physiol Gastrointest Liver Physiol* 267: G442–G451, 1994.
32. **Hofer AM, Machen TE.** Technique for in situ measurement of calcium in intracellular inositol 1,4,5-trisphosphate-sensitive stores using the fluorescent indicator mag-fura-2. *Proc Natl Acad Sci USA* 90: 2598–2602, 1993.
33. **Ishihara R, Iishi H, Sakai N, Yano H, Uedo N, Narahara H, Iseki K, Mikuni T, Ishiguro S, Tatsuta M.** Polaprezinc attenuates *Helicobacter pylori*-associated gastritis in Mongolian gerbils. *Helicobacter* 7: 384–389, 2002.
34. **Jouaville LS, Pinton P, Bastianutto C, Rutter GA, Rizzuto R.** Regulation of mitochondrial ATP synthesis by calcium: evidence for a long-term metabolic priming. *Proc Natl Acad Sci USA* 96: 13807–13812, 1999.
35. **Kress GJ, Dineley KE, Reynolds IJ.** The relationship between intracellular free iron and cell injury in cultured neurons, astrocytes, and oligodendrocytes. *J Neurosci* 22: 5848–5855, 2002.
36. **Laemmli UK.** Cleavage of structural proteins during the assembly of the head of bacteriophage T4. *Nature* 227: 680–685, 1970.
37. **Maret W.** Crosstalk of the group IIa and IIb metals calcium and zinc in cellular signaling. *Proc Natl Acad Sci USA* 98: 12325–12327, 2001.
38. **Maret W.** Zinc and sulfur: a critical biological partnership. *Biochemistry* 43: 3301–3309, 2004.
39. **Mearow KM, Thilander BG, Khan I, Garfield RE, Grover AK.** In situ hybridization and immunocytochemical localization of SERCA2 encoded Ca^{2+} pump in rabbit heart and stomach. *Mol Cell Biochem* 121: 155–165, 1993.
40. **Naito Y, Yoshikawa T.** Molecular and cellular mechanisms involved in *Helicobacter pylori*-induced inflammation and oxidative stress. *Free Radic Biol Med* 33: 323–336, 2002.
41. **Negulescu PA, Machen TE.** Intracellular ion activities and membrane transport in parietal cells measured with fluorescent dyes. *Methods Enzymol* 192: 38–81, 1990.
42. **Orrenius S, Zhivotovsky B, Nicotera P.** Regulation of cell death: the calcium-apoptosis link. *Nat Rev Mol Cell Biol* 4: 552–565, 2003.
43. **Parekh AB.** Store-operated Ca^{2+} entry: dynamic interplay between endoplasmic reticulum, mitochondria and plasma membrane. *J Physiol* 547: 333–348, 2003.
44. **Peskin AV, Winterbourn CC.** Kinetics of the reactions of hypochlorous acid and amino acid chloramines with thiols, methionine, and ascorbate. *Free Radic Biol Med* 30: 572–579, 2001.
45. **Rizzuto R, Bernardi P, Pozzan T.** Mitochondria as all-round players of the calcium game. *J Physiol* 529: 37–47, 2000.

46. **Ruiz FA, Lea CR, Oldfield E, Docampo R.** Human platelet dense granules contain polyphosphate and are similar to acidocalcisomes of bacteria and unicellular eukaryotes. *J Biol Chem* 279: 44250–44257, 2004.
47. **Sen CK.** Cellular thiols and redox-regulated signal transduction. *Curr Top Cell Regul* 36: 1–30, 2000.
48. **Sensi SL, Ton-That D, Sullivan PG, Jonas EA, Gee KR, Kaczmarek LK, Weiss JH.** Modulation of mitochondrial function by endogenous Zn^{2+} pools. *Proc Natl Acad Sci USA* 100: 6157–6162, 2003.
49. **St Croix CM, Wasserloos KJ, Dineley KE, Reynolds IJ, Levitan ES, Pitt BR.** Nitric oxide-induced changes in intracellular zinc homeostasis are mediated by metallothionein/thionein. *Am J Physiol Lung Cell Mol Physiol* 282: L185–L192, 2002.
50. **Suzuki M, Miura S, Suematsu M, Fukumura D, Kurose I, Suzuki H, Kai A, Kudoh Y, Ohashi M, Tsuchiya M.** *Helicobacter pylori*-associated ammonia production enhances neutrophil-dependent gastric mucosal injury. *Am J Physiol Gastrointest Liver Physiol* 263: G719–G725, 1992.
51. **Suzuki YJ, Forman HJ, Sevanian A.** Oxidants as stimulators of signal transduction. *Free Radic Biol Med* 22: 269–285, 1997.
52. **Tamai H, Kachur JF, Baron DA, Grisham MB, Gaginella TS.** Monochloramine, a neutrophil-derived oxidant, stimulates rat colonic secretion. *J Pharmacol Exp Ther* 257: 887–894, 1991.
53. **Thomas EL, Jefferson MM, Grisham MB.** Myeloperoxidase-catalyzed incorporation of amines into proteins: role of hypochlorous acid and dichloramines. *Biochemistry* 21: 6299–6308, 1982.
54. **Turan B, Fliss H, Desilets M.** Oxidants increase intracellular free Zn^{2+} concentration in rabbit ventricular myocytes. *Am J Physiol Heart Circ Physiol* 272: H2095–H2106, 1997.
55. **Yajima N, Hiraishi H, Yamaguchi N, Ishida M, Shimada T, Terano A.** Monochloramine-induced cytolysis to cultured gastric mucosal cells. *J Lab Clin Med* 134: 372–377, 1999.
56. **Yoshikawa T, Naito Y.** The role of neutrophils and inflammation in gastric mucosal injury. *Free Radic Res* 33: 785–794, 2000.